Scalar density fluctuation at critical end point in NJL model

H. Fujii*
Institute of Physics, University of Tokyo
3-8-1 Komaba, Meguro, Tokyo 153-8902, Japan
(February 1, 2008)

Soft mode near the critical end point in the phase diagram of two-flavor Nambu–Jona-Lasinio (NJL) model is investigated within the leading $1/N_c$ approximation with N_c being the number of the colors. It is explicitly shown by studying the spectral function of the scalar channel that the relevant soft mode is the scalar density fluctuation, which is coupled with the quark number density, while the sigma meson mode stays massive.

12.38.-t, 24.85.+p, 05.70.-a, 64.70.-p

arXiv:hep-ph/0302167v2 7 Apr 2003

I. INTRODUCTION

Existence of critical end point (CEP) in the QCD phase diagram is recently suggested in several works [1–5], and its implications to the phenomena in the heavy ion physics are intensively discussed in order to identify its location experimentally [6–14].

The critical end point is the end point of the phase boundary determined by the first order phase transition. The nature of this point has been discussed so far mainly from the viewpoint of the chiral symmetry. The order parameter is the scalar quark condensate, $\langle\bar{q}q\rangle \sim \sigma$, which strictly vanishes in the Wigner phase in the chiral limit. At the CEP in question the phase transition necessarily becomes of second order even with the non-zero current quark mass $m \neq 0$, and the curvature of the free energy w.r.t. the scalar field should vanish. This fact immediately implies the emergence of a gapless excitation in the scalar channel. The existence of this second-order transition, however, is accidental in the sense that no symmetry change of the ground state is accompanied with this transition. In fact the finite current quark mass, which breaks the chiral symmetry explicitly, results in the non-vanishing scalar condensate at any point in the plane of the temperature and the quark chemical potential $(T-\mu)$, in contrast to the case with $m = 0$. Only its fluctuation around the equilibrium value becomes unstable at the CEP. This "accidental" instability is not related to any symmetry of the system.

Even in the chiral symmetric world with $m = 0$, presence of the tricritical point (TCP), which is the counterpart of the CEP, is not necessarily required by the spontaneous breaking of the chiral symmetry. The change of the symmetry realization of the system constitutes a boundary line in the phase diagram, on which the first-order or the second-order transition occurs. The soft mode for the chiral breaking is known as sigma meson, and it becomes gapless on the second-order line so as to recover the chiral symmetry together with the Goldstone pion. The TCP exists as a point separating the boundary line into the segments of the first-order and the second-order transitions, depending on the parameters T and μ. What kind of singular behavior will appear additionally at this TCP, where the sigma mode is already gapless?

The most natural expectation may be that the density fluctuation becomes soft near the CEP because it is the end point of the first order transition which accompanies the density gap caused by the strong attraction between the quarks. The aim of this paper is to prove this scenario explicitly within the NJL model [15,16] in the leading $1/N_c$ approximation, and to show that the nature of the CEP is rather similar to the liquid–gas critical point than the chiral transition. The density fluctuation discussed here will be the collective motion of the particle-hole-like excitations. One should note that this density fluctuation has a space–like dispersion relation from the kinematical reason. Thus, we will be forced to investigate the mode spectrum with this kinematics. If this is the case, some of the implications discussed before in the literature [6,10,13] must be reconsidered in relation to the heavy ion experiments; at the CEP the sigma meson, which is the chiral partner of the pion, can remain massive. One should study the observables distinctive of the space-like density fluctuations, rather than the particle production processes with the time–like kinematics.

The nature of the phase transition is insensitive to the microscopic structure of the system. The most important ingredients which determine the nature of the transition are the dimension of the system, the symmetry of the

*Email: hfujii@phys.c.u-tokyo.ac.jp

interactions or the dimension of the order parameter(s), and the range of the interactions. If the study is extended to include the dynamical nature, these universarity classes for the static properties split into subclasses depending on the existence of the conservation law(s) and mode-mode coupling(s), and so on [17]. It may be, therefore, perilous to utilize (e.g.) the Ising model results in order to speculate the dynamical nature of the QCD phase transition. With this caution in mind we employ a concrete model of the quarks in this paper to study the dynamical properties of the phase transition at the CEP.

We use the NJL model here as a simple model which can describe the CEP as well as the chiral phase transition of the quark system. One of the advantages of the use of the NJL model is that the bosonic collective modes of the system are easily and explicitly calculated. Our main conclusions are expected to hold irrespective of the details of the model employed here. We should still keep cautious, however, because this model lacks the long-range nature of the color interactions, and the gluonic degrees of freedom at all. In this paper we restrict our discussion only for the second order phase transition at the CEP ($m \neq 0$). More complete analysis treating the TCP, and the vector and entropy density fluctuations, will be reported in the forthcoming paper [18] in the NJL model as well as in the linear sigma model.

This paper is organized as follows. In §II the behavior of the susceptibilities in the NJL phase transition is discussed. In §III the spectral function of the scalar mode is investigated in some details and the relevant slow mode is explicitly identified as the scalar density fluctuation. §IV is devoted to summary.

II. SUSCEPTIBILITIES IN THE NJL PHASE TRANSITION

We use the simplest version of the NJL model with two flavors ($N_f = 2$) [19] whose laglangian is, with obvious notations,

$$\mathcal{L} = \bar{q}(i\partial\!\!\!/ - m)q + g[(\bar{q}q)^2 + (\bar{q}i\gamma_5\tau^a q)^2]. \tag{1}$$

After introducing the auxiliary fields σ and π for $\bar{q}q$ and $\bar{q}i\gamma_5\tau^a q$ in a standard way, the system pressure at finite temperature T and finite quark chemical potential μ is written, within the mean–field approximation with σ=const and π=0, as

$$\frac{1}{\nu}P(T,\mu,m;\sigma) = \int \frac{d^3k}{(2\pi)^3}[E - T\ln(1-n_-) - T\ln(1-n_+)] - \frac{1}{4}\frac{1}{g\nu}\sigma^2, \tag{2}$$

where $n_\pm = (e^{\beta(E\mp\mu)}+1)^{-1}$, $E = \sqrt{M^2+\mathbf{k}^2}$, $M = m - \sigma$, and $\nu = 2N_fN_c$ is the number of the quark species. This expression corresponds to the leading $1/N_c$ approximation with gN_c being $O(1)$, though we set $N_c = 3$ in the following. From the pressure $P(T,\mu,m;\sigma)$ we can calculate all the thermodynamical quantities.

The ground state at (T,μ) satisfies the stationary condition for σ, which yields the gap (saddle point) equation

$$\int \frac{d^3k}{(2\pi)^3}\frac{M}{E}(1-n_--n_+) + \frac{1}{2}\frac{1}{g\nu}\sigma = 0. \tag{3}$$

We define the curvature of the potential w.r.t. the scalar field at the saddle point

$$\begin{aligned} -\frac{\partial^2 P}{\partial\sigma^2} &\equiv K \\ &= \frac{1}{2g} - \nu\int\frac{d^3k}{(2\pi)^3}\frac{1}{E}(1-n_--n_+) + \nu\int\frac{d^3k}{(2\pi)^3}\frac{M^2}{E^2}\left(\frac{1-n_--n_+}{E} + n_-' + n_+'\right) \\ &= \frac{1}{2g} - \chi^{(0)}_{mm} \geq 0 \end{aligned} \tag{4}$$

with $n_\pm' = \partial n_\pm/\partial E$. The last inequality must be satisfied according to thermodynamical stability. The occurrence of the second order phase transition is signaled by the vanishing curvature, $K = 0$. Furthermore, we notice from Eq. (4) together with the gap equation, that $K \sim M^2 \to 0$ at the second order chiral transition approached from the lower temperature or density. As we shall see later, K is proportional to the inverse propagator of the static scalar mode in the long wave length limit.

The susceptibilities $\chi_{ab} = \partial^2 P/\partial a\partial b$ $(a,b = T,\mu,m)$ are very important to characterize the nature of the phase transition [20,21]. In our approximation these susceptibilities have a simple common structure as

$$\chi_{ab} = \chi^{(0)}_{am}\frac{1}{K}\chi^{(0)}_{mb} + \chi^{(0)}_{ab}, \tag{5}$$

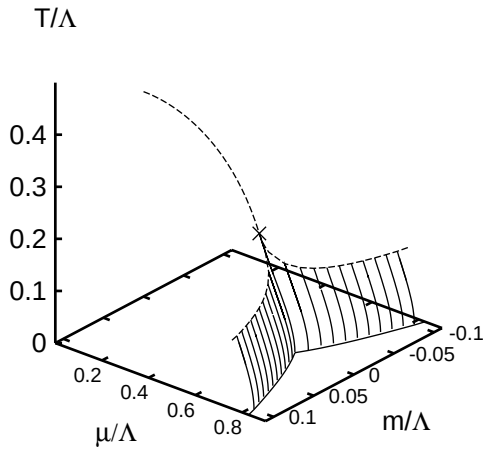

FIG. 1. Calculated phase diagram of the NJL model. The transition line of the second order is drawn in the dashed line. The phase boundary of the first order transition constitutes a surface shown by hatch. The cross indicates the tricritical point, where three lines of second order transition meet.

where $\chi^{(0)}_{ab}$ are the non-singular parts of the susceptibilities and equal to those of the free quark gas of mass M. From this expression we find that all divergences at the second order phase transition originate from the flatness of the potential curvature $K \to 0$. One should note here that the mixing of the susceptibilities with the scalar mode $\chi^{(0)}_{am}$ $(a = T, \mu)$ is proportional to M. Thus, at the chiral phase transition where $m = 0$, the would-be singular parts of χ_{ab} $(a, b = T, \mu)$ involving the factor $1/K$, are less singular than χ_{mm}. Actually they remain finite (vanish) if the transition point (T_c, μ_c) is approached from the broken (symmetric) phase because the constituent quark mass M vanishes on the boundary and in the symmetric phase. On the other hand, at the CEP $(m \neq 0)$, M stays finite and the critical behavior of these susceptibilities is essentially the same as χ_{mm}. This argument is consistent with the analysis based on the general properties of the Landau free energy with the tricritical point [12], as it should be.

The discussion can be extended a little bit further by changing the thermodynamical variables. Let us choose the quark number density ρ_q as an independent variable instead of μ. Then the scalar susceptibility with fixed quark number density is related to the susceptibilities given in Eq. (5) via

$$\chi_{mm}(T, \rho_q) = \frac{1}{\chi_{\mu\mu}}(\chi_{mm}\chi_{\mu\mu} - \chi^2_{m\mu}) = \frac{(\chi^{(0)}_{mm}\chi^{(0)}_{\mu\mu} - {\chi^{(0)}_{m\mu}}^2)(1 + \frac{1}{K}\chi^{(0)}_{mm})}{\chi^{(0)}_{\mu\mu} + \chi^{(0)}_{\mu m}\frac{1}{K}\chi^{(0)}_{m\mu}}. \tag{6}$$

We find that the K^{-2} term is canceled out in the numerator. At the chiral phase transition we already pointed out that $\chi_{\mu\mu} \to$ constant, and then the scalar susceptibility with the fixed quark number density $\chi_{mm}(T, \rho_q)$ diverges in the same way as χ_{mm}. There the vector susceptibility is decoupled from the scalar one as $\chi^{(0)}_{m\mu} \sim M \to 0$. In case of the CEP which we are concerned about, however, $\chi^{(0)}_{m\mu}$ remains finite, and the denominator and the numerator in Eq. (6) diverges in the same way as $1/K$, which results in the finite scalar susceptibility. This demonstrates that the coupling with the number density fluctuation is essential for the divergence accompanied by the CEP. Similarly the thermal susceptibility with fixed quark number density, $\chi_{TT}(T, \rho_q) = (\chi_{TT}\chi_{\mu\mu} - \chi^2_{\mu T})/\chi_{\mu\mu}$, does not diverge at the CEP, but χ_{TT} in Eq. (5) does.

This situation is completely analogous to the thermal susceptibility or the specific heat in the liquid–gas phase transition, where the density gap between two phases is identified as the order parameter. The specific heat at constant pressure and the isothermal compressibility diverge like $|T - T_c|^{-\gamma}$ at the critical point. Once we keep the number (entropy) density fixed, however, the specific heat at constant volume (the isentropic compressibility) remains finite or diverges only weakly like $|T - T_c|^{-\alpha}$) [22].

The NJL model has two fundamental parameters: the coupling constant g and the cutoff Λ. The "physical values" of these parameters are usually fixed so as to reproduce the chiral quark condensate $\langle\bar{q}q\rangle$ and the pion decay constant f_π. Taking the three–momentum cutoff scheme, the critical value $g_c\Lambda^2$ for the spontaneous symmetry breaking in the

vacuum is readily found as $g_c\Lambda^2 = \frac{2\pi^2}{\nu} = 1.64\cdots$ in the chiral limit ($m = 0$). There is also a critical value for the appearance of the TCP, which value is obtained as $g_{TCP}\Lambda^2 = \frac{2\pi^2}{\nu}\frac{1}{1-e^{-2}} = 1.90\cdots$ from the condition that the σ^2– and σ^4–terms simultaneously vanish in the pressure $P(T,\mu,0;\sigma)$. It is interesting to note that the TCP must appear with the finite chemical potential $(T/\Lambda, \mu/\Lambda) = (0, 1/e)$ at $g = g_{TCP}$ and that it approaches the T-axis asymptotically as g getting larger; this fact proves that the TCP is only possible at finite number density in our model.

In this paper, for demonstration, we set $g\Lambda^2 = 2.5$, and all other dimensionful quantities will be measured in the unit of Λ. The phase diagram of the NJL model in the mean field approximation is shown in Fig. 1. This shares the well-known structure of the phase diagram possessing a tricritical point [23]. The character of this diagram around the TCP is studied using the Landau free energy and the Schwinger-Dyson equation of the ladder QCD in Ref. [12]. Their results on the quark mass dependence of the boundary curves and the behavior of the susceptibilities are consistent with those in NJL calculations [18], because the symmetry and order parameters of the system are the same.

III. RESPONSE FUNCTIONS AND MESON SPECTRUM

In order to clarify the structure of the relevant modes for the phase transition, we should investigate the spectral functions [24–27]. Using the linear response theory, we first calculate the response functions in the relevant channels, whose imaginary parts give rise to the mode spectra.

Let us assume artificially small deviations of the chemical potential and the current quark mass, $\tilde{\mu}, \tilde{m}$, from their equilibrium and physical values, respectively. The response functions for these disturbances are calculated as

$$\chi_{ab}(iq_4,\mathbf{q}) = \Pi_{ab}(iq_4,\mathbf{q}) + \Pi_{am}(iq_4,\mathbf{q})\frac{1}{1-2g\Pi_{mm}(iq_4,\mathbf{q})}2g\Pi_{mb}(iq_4,\mathbf{q}), \qquad (a,b=\mu,m). \tag{7}$$

Here the polarizations are defined with the imaginary–time quark propagator $\mathcal{S}$ as

$$\Pi_{mm}(iq_4,\mathbf{q}) = -\int\frac{d^3k}{(2\pi)^3}T\sum_n tr_{\rm fcD}\mathcal{S}(\tilde{k})\mathcal{S}(\tilde{k}-q), \tag{8}$$

$$\Pi_{\mu\mu}(iq_4,\mathbf{q}) = -\int\frac{d^3k}{(2\pi)^3}T\sum_n tr_{\rm fcD}\mathcal{S}(\tilde{k})i\gamma_4\mathcal{S}(\tilde{k}-q)i\gamma_4, \tag{9}$$

$$\Pi_{m\mu}(iq_4,\mathbf{q}) = -\int\frac{d^3k}{(2\pi)^3}T\sum_n tr_{\rm fcD}\mathcal{S}(\tilde{k})\mathcal{S}(\tilde{k}-q)i\gamma_4, \tag{10}$$

where $q_4 = 2l\pi T$ ($l \in \mathbb{Z}$) is the Matsubara frequancy of the bosonic mode, $\tilde{k} = (\mathbf{k}, k_4+i\mu) = (\mathbf{k}, -\omega_n+i\mu)$ is the quark loop momentum with $\omega_n = (2n+1)\pi T$ ($n \in \mathbb{Z}$), and the traces are taken over the flavor, color and Dirac indices. The real–time response function is obtained by an analytic continuation, which is simply achieved by a replacement $iq_4 \to q_0+i\epsilon$ after the Matsubara sum. These response functions in the static case should reduce to the susceptibilities in Eq. (5). From this fact we find that the static polarization $\Pi_{ab}(0,\mathbf{q}\to\mathbf{0})$ are the free susceptibilities $\chi^{(0)}_{ab}(\mathbf{q}\to\mathbf{0})$, which can be also confirmed by explicit calculations.

The common denominator, $\frac{1}{2g} - \Pi_{mm}(q_0,\mathbf{q})$, is proportional to the inverse of the scalar response function, and its static value coincides with the potential curvature K in the long wave length limit. Diagrammatically, this denominator corresponds to the sum of the bubble diagrams in the scalar channel. The gapless excitation mode which is responsible for the appearance of the CEP and for all divergences of the scalar, vector and entropy fluctuations through the coupling, must be contained in the spectrum of this bubble diagram.

The only task we have to do, therefore, is to investigate the spectrum of the scalar excitation determined by the condition

$$\chi^{-1}_{mm} \propto \frac{1}{2g} - \Pi_{mm}(q_0,\mathbf{q}) = \frac{1}{2g} - J(\mathbf{q}) + (4M^2-q^2)I(q_0,\mathbf{q}) = 0, \tag{11}$$

where

$$\begin{aligned} I(iq_4,\mathbf{q}) &= \nu\int\frac{d^3k}{(2\pi)^3}T\sum_n\frac{1}{(\tilde{k}^2+M^2)((\tilde{k}-q)^2+M^2)} \\ &= \nu\int^{k_{\max}}\frac{d^3k}{(2\pi)^3}\frac{-1}{4E_1E_2}\left[\frac{1-n_{+1}-n_{-2}}{iq_4-E_1-E_2} - \frac{n_{-1}-n_{-2}}{iq_4+E_1-E_2} + \frac{n_{+1}-n_{+2}}{iq_4-E_1+E_2} - \frac{1-n_{-1}-n_{+2}}{iq_4+E_1+E_2}\right], \end{aligned} \tag{12}$$

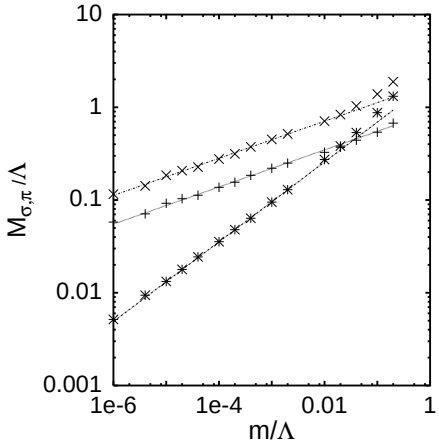

FIG. 2. Sigma ($\times$) and pion ($*$) masses $M_{\sigma,\pi}$ at the CEP as functions of the current quark mass m. The constituent quark mass M ($+$) is displayed as well.

and

$$J(\mathbf{q}) = \nu \int \frac{d^3k}{(2\pi)^3} \left(\frac{1-n_{-1}-n_{+1}}{2E_1} + \frac{1-n_{-2}-n_{+2}}{2E_2} \right)$$
$$= \frac{\nu}{2\pi^2|\mathbf{q}|} \int_0^{k_{\max}} dk k \left[\omega_{\max} - \omega_{\min} + T \ln \frac{(1+e^{-(\omega_{\max}-\mu)/T})(1+e^{-(\omega_{\max}+\mu)/T})}{(1+e^{-(\omega_{\min}-\mu)/T})(1+e^{-(\omega_{\min}+\mu)/T})} \right] \tag{13}$$

with $E_{1,2} = \sqrt{M^2 + (\mathbf{k} \pm \mathbf{q}/2)^2}$, $n_{\pm 1,2} = n_\pm(E_{1,2})$ and $\omega_{\max,\min} = \sqrt{M^2 + \mathbf{k}^2 + \mathbf{q}^2/4 \pm |\mathbf{q}||\mathbf{k}|}$. In these equations we shifted the three momentum $\mathbf{k}$ to make the integral more symmetric and chose a simple convention of the cutoff for the mode with finite momentum $\mathbf{q}$ as $k_{\max}^2 = \Lambda^2 - \mathbf{q}^2/4$. The stable mode should be obtained as a real solution of Eq. (11). The unstable, resonance mode will be found as a complex-valued solution in the unphysical lower half plane of q_0.

The function $I(q_0, \mathbf{q})$ is elementary in the thermal field theory [28]. By noting $1-n_+-n_- = (1-n_-)(1-n_+)-n_-n_+$ (pair creation $-$ annihilation) and $n_{-1}-n_{-2} = (1-n_{-2})n_{-1} - (1-n_{-1})n_{-2}$ (emission $-$ absorption) and so on, we find that the first and last terms in Eq. (12) are contributions of the time–like spectrum while the second and third come from the space–like spectrum in the spectral representation for $I(q_0, \mathbf{q})$. It may be instructive to note here that two limits of the function $I(q_0, \mathbf{q})$ are different:

$$I(0, \mathbf{q} \to \mathbf{0}) = \nu \int \frac{d^3k}{(2\pi)^3} \frac{1}{4E^2} \left(\frac{1-n_+-n_-}{E} + n'_- + n'_+ \right), \tag{14}$$

$$I(q_0 \to 0, \mathbf{0}) = \nu \int \frac{d^3k}{(2\pi)^3} \frac{1}{4E^2} \frac{1-n_+-n_-}{E}. \tag{15}$$

The difference is due to the space-like mode contribution; in the first limiting procedure I has the space-like mode contribution while in the second case we don't see it. This is the origin of the fact that the massive sigma meson and the zero curvature of the free energy can cope with each other [See also Eq. (4)].

A. Sigma and pion masses

First we study the excitation energy of the massive mode, which is continuously connected to the sigma meson in the vacuum as the parameters (T, μ) are varied. To this end we set $q = (q_0, \mathbf{q}) = (\omega, \mathbf{0})$, following the usual calculation of the sigma meson mass in the vacuum. Then $J = \nu \int \frac{d^3k}{(2\pi)^3}(1-n_--n_+)/E$, and together with the gap equation we recover the well-known condition to determine the sigma energy,

$$\frac{1}{2g}\frac{m}{M} + (4M^2 - \omega^2) I(\omega, \mathbf{0}) = 0. \tag{16}$$

Similarly for the pions,

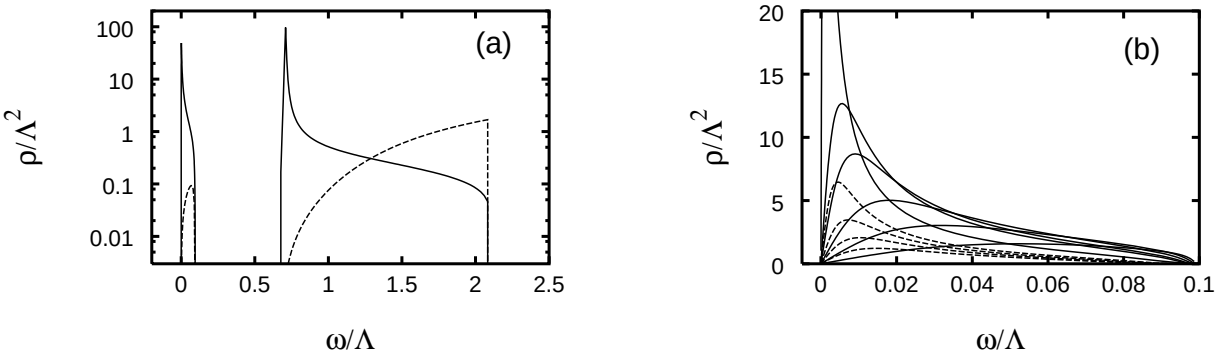

FIG. 3. Calculated spectral function in the scalar mode with $(T/\Lambda, m/\Lambda, |\mathbf{q}|/\Lambda) = (0.14985, 0.01, 0.1)$. (a) Profile at the CEP (solid line) together with the free spectrum (dashed line). (b) Profile in the space–line region with varying the chemical potential as μ/Λ =0.59, 0.58, 0.575, 0.572, 0.571, 0.57006 ($=\mu_c$) (solid lines), 0.5682, 0.5652, 0.56, 0.55 (dashed lines).

$$\frac{1}{2g}\frac{m}{M} - \omega^2 I(\omega, \mathbf{0}) = 0. \tag{17}$$

In the chiral limit the energies of the stopped sigma and pion are $\omega = 2M$ and 0, respectively, which fact is known as Nambu relation [19] in the symmetry-broken phase.

At the CEP, on the other hand, the constituent quark mass M remains massive due to the non-zero current quark mass, and therefore we expect the sigma meson has a finite energy gap as a remnant of the Nambu relation. From the argument using the Landau free energy, M is expected to scale with $m^{1/5}$ at the CEP [12,23]. With neglecting the imaginary part of I, we numerically confirm this behavior, in Fig. 2, for the sigma mass M_σ determined by Eq. (16) as well as the constituent quark mass M. The pion mass will be proportional to $(m/M)^{1/2} \sim m^{2/5}$ from Eq. (17), and it is numerically found as $\sim m^{0.43}$. It should be stressed here that the massive behavior of the sigma is quite normal from the viewpoint of the Nambu relation, and does not introduce any problem in the description of the phase transition. Actually it is found that the massive sigma and the vanishing curvature take place at the same time at the CEP in the NJL model [29], as well as in the linear sigma model [30], in the mean–field approximation.

B. Spectrum of the scalar mode and the phase transition

As we explained in Introduction, we expect that the instability occurs in the almost static and long wave length region in the scalar density fluctuation (as well as in the vector and entropy fluctuations through the coupling). In order to investigate the spectrum of the relevant modes in the transition at the CEP, we must keep the momentum $\mathbf{q}$ finite.

The spectral function of the scalar mode, $\rho(\omega, \mathbf{q}) = 2\mathrm{Im}\chi_{mm}(\omega, \mathbf{q})$, is explicitly written as

$$\frac{1}{2}\rho(\omega, \mathbf{q}) = \mathrm{Im}\chi_{mm}(\omega, \mathbf{q}) = \frac{-(\frac{1}{2g})^2(4M^2 - q^2)\mathrm{Im}I(\omega, \mathbf{q})}{[\frac{1}{2g} - J(\mathbf{q}) + (4M^2 - q^2)\mathrm{Re}I(\omega, \mathbf{q})]^2 + [(4M^2 - q^2)\mathrm{Im}I(\omega, \mathbf{q})]^2} \tag{18}$$

up to delta functions coming from possible non-decaying stable modes. We noticed previously that $\Pi_{mm}(\omega, \mathbf{q})$ is the scalar response function of the free quark gas of mass M, whose imaginary part

$$\frac{1}{2}\rho^{(0)}(\omega, \mathbf{q}) = \mathrm{Im}\Pi_{mm}(\omega, \mathbf{q}) = -(4M^2 - q^2)\mathrm{Im}I(\omega, \mathbf{q}) \tag{19}$$

is the scalar channel spectrum of the uncorrelated quarks. These spectral functions have the support in the time-like region with $q^2 = \omega^2 - \mathbf{q}^2 > 4M^2$ and in the space-like region with $q^2 = \omega^2 - \mathbf{q}^2 < 0$.

In the numerical calculation presented here, we fix the current quark mass to $m/\Lambda = 0.01$ for definiteness. The corresponding CEP locates at $(T/\Lambda, \mu/\Lambda) = (0.14985, 0.57006)$. The spectrum of $\chi_{mm}(\omega, \mathbf{q})$ with $|\mathbf{q}|/\Lambda = 0.1$ is shown in Fig. 3 (a), in which we see two sharp peaks at very low frequency and around $2M$ ($M/\Lambda = 0.331$). The free spectrum is also displayed for comparison. It is understood that the scalar channel attraction, which is encoded as a bubble sum in the denominator in Eq. (7) or in Eq. (18), changes the structure of the spectrum dramatically. The resulting scalar mode develops two distinct branches. The higher frequency peak corresponds to the sigma meson while the lower one appearing in the space–like region ($\omega < |\mathbf{q}|$) is the scalar density fluctuating mode which we expect is

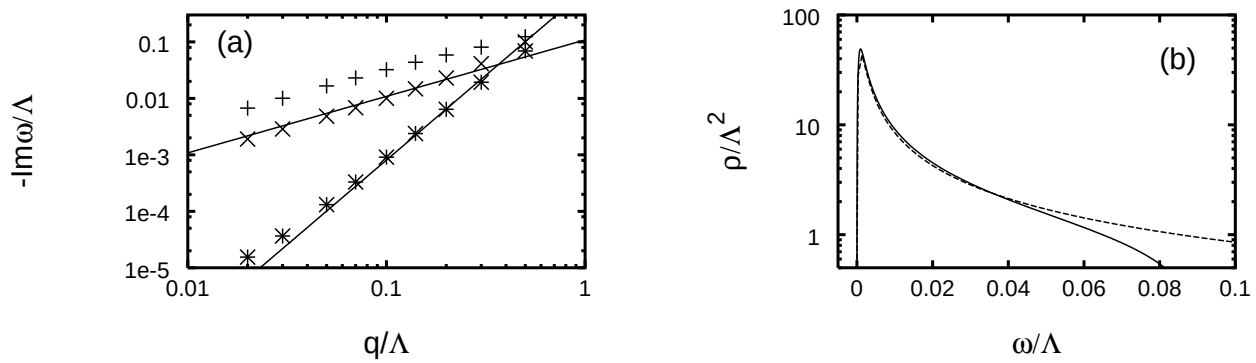

FIG. 4. (a) The pole position of $\chi_{mm}(\omega, \mathbf{q})$ as a function of $|\mathbf{q}|/\Lambda$ for the CEP ($*$), a lower density ($\mu/\Lambda = 0.56$, $\times$), and a higher density ($\mu/\Lambda = 0.58$, $+$), together with the straight lines ($\propto |\mathbf{q}|^3$ and $|\mathbf{q}|^1$). (b) Spectral function of the single pole form Eq. (21) (dashed line) in the space-like region at the CEP is compared with the numerical result (18) (solid line) with $|\mathbf{q}|/\Lambda = 0.1$.

responsible for the second order phase transition. Actually the latter peak diverges as $\mathbf{q} \to \mathbf{0}$. We study the structure of the peak in the space–like region near the CEP in more detail in Fig. 3 (b). The enhancement of the spectrum is clearly demonstrated as the CEP is approached from the higher densities, $\mu/\Lambda = 0.59, 0.58, 0.575, 0.572, 0.571$ (solid lines), and also from the lower $\mu/\Lambda = 0.55, 0.56, 0.5652, 0.5682$ (dashed lines) with $\mu_c/\Lambda = 0.57006$.

We searched the pole in the unphysical lower half plane of ω [25–27], responsible for this peak. Indeed the pole is found on the negative imaginary axis as shown in Fig. 4 (a). We observed that the pole is moving toward the origin as decreasing the momentum $\mathbf{q}$. Even in the non-critical case there is a pole on the negative imaginary axis and it moves toward the origin as $\mathbf{q} \to \mathbf{0}$, too. The difference between the critical and non-critical cases exists in the exponent of the $\mathbf{q}$-dependence; the pole position goes to zero as $|\mathbf{q}|^3$ in the critical case while on the other hand it behaves like $|\mathbf{q}|^1$ for non-critical case.

This result can be understood if one notes that in the static limit of the "sound" mode, $\omega \to 0$ with $u \equiv \omega/|\mathbf{q}| < 1$ fixed, the function I has the form ($v = k/E$) [31]

$$I(u) = I(0, |\mathbf{q}| \to 0) - \frac{\nu}{2\pi^2} \int_0^\Lambda dk (n'_- + n'_+) \frac{uv}{8} \left(\ln \left| \frac{v+u}{v-u} \right| - \mathrm{i}\pi\theta(1 - \frac{u}{v}) \right), \tag{20}$$

whose imaginary part is proportional to $u = \omega/|\mathbf{q}|$ for small u. This imaginary part physically expresses the damping of the scalar "sound" mode in the quark gas. Then the response function with the space-like kinematics near the CEP may be approximated with

$$\chi_{mm}(\omega, \mathbf{q}) \sim \frac{\mathrm{Re}\Pi_{mm}(0, \mathbf{q})}{-\mathrm{i}2g\mathrm{Im}\Pi_{mm}(\omega, \mathbf{q}) + (1 - 2g\mathrm{Re}\Pi_{mm}(0, \mathbf{q}))} = \frac{1}{-\mathrm{i}\frac{\omega}{\lambda(\mathbf{q})} + \chi^{-1}_{mm}(\mathbf{q})} = \frac{\lambda(\mathbf{q})}{-\mathrm{i}\omega + \omega_c(\mathbf{q})}, \tag{21}$$

where $\chi_{mm}(\mathbf{q})$ is the scalar susceptibility, and $\omega_c(\mathbf{q}) \equiv \chi^{-1}_{mm}(\mathbf{q})\lambda(\mathbf{q})$. Here we expect $\lambda(\mathbf{q}) \propto |\mathbf{q}|$, and numerically confirmed it. The susceptibility behaves as $\chi^{-1}_{mm}(\mathbf{q} \to \mathbf{0}) \propto |\mathbf{q}|^2$ at the CEP, but stays constant in non-critical region. This difference of the $\mathbf{q}$-dependence of $\chi_{mm}(\mathbf{q})$ alters the exponent of the $\mathbf{q}$-dependence of the pole position, as described above and shown in Fig. 4 (a).

We confirmed in Fig. 4 (b) that the ω-dependence of the response function at the CEP is well reproduced in the single pole form (21) with the values $(\omega_c(\mathbf{q}), \chi^{-1}_{mm}(\mathbf{q})) = (0.90925 \cdot 10^{-3}, 0.21300 \cdot 10^{-1})$ obtained in our numerical pole search. The deviation seen around $\omega/\Lambda \sim 0.1$ is due to the lack of the kinematical cutoff to confine the spectrum inside the space-like region when we use the single pole form (21). We also checked that the response functions for the non-critical case near the CEP can be also described with the single pole form fairly well. Incidentally it is immediately seen that the form of (21) has the different limits around the origin: if one take the $\mathbf{q} \to \mathbf{0}$ limit first, $\chi_{mm}(\omega, 0) \to 0$. On the other hand, $\chi_{mm}(0, \mathbf{q}) = \chi_{mm}(\mathbf{q}) \to \infty$ as $\mathbf{q} \to \mathbf{0}$.

The typical slow frequency of the system near the CEP is $\omega_c(\mathbf{q}) = \chi^{-1}_{mm}(\mathbf{q})\lambda(\mathbf{q})$. This means that we reconfirmed the conventional theory of dynamical critical phenomena [32] in the form of Eq. (21): the divergence of the susceptibility is directly related to the critical slowing down of the response of the system to the external disturbance. The exponent of the dynamical scaling in our model will be equal to 3.

IV. SUMMARY

In this paper we have explicitly shown that there are two branches in the scalar mode in the NJL model at finite (T, μ). The sigma meson mode stays massive at the CEP, following the approximate relation, $M_\sigma \sim 2M$. The other mode is the scalar density fluctuation which becomes soft and relevant near the CEP. This result is perfectly consistent with the description of the second order phase transition using the Landau free energy. The first observation of the massive sigma at the CEP was done in Ref. [10] although it led the authors to a somewhat confused discussion.

All the susceptibilities $\chi_{ab}(a, b = T, \mu, m)$ are found divergent at the CEP due to the flatness of the potential curvature, $K \to 0$. The importance of the density fluctuation at the CEP is shown by considering the number-density-fixed susceptibility, $\chi_{mm}(T, \rho_q)$. It no longer diverges at the CEP, but still does at the chiral phase transition. This situation at the CEP is quite similar to the liquid–gas phase transition, where the density difference between two phases is identified as the relevant order parameter.

From our analysis we conclude that the CEP line in Fig. 1 denotes the second order phase transition characterized by the instability of the density fluctuations. Two lines of the CEP and the line of the second order chiral transition meet at the TCP (therefore tricritical), where we expect that the sigma meson and the density fluctuation mode become unstable at the same time. Although some readers could expect our conclusion from the beginning, there are confusions on this point in the literature [6,10,13] and one of our contributions is to clarify the importance of the density fluctuation explicitly using a concrete model for the CEP of a quark system.

As for the experimental signatures of the CEP one should investigate first the implications of the anomalous fluctuations [7,8,12,14,33–35] of the baryon number, entropy, and scalar densities. One should be careful that the modification of the density fluctuations with the space–like momentum does not affect directly the spectrum of the particle production modes, like $\sigma \to \pi\pi, \bar{l}l, \gamma\gamma$, because of the kinematical mismatching.

ACKNOWLEDGMENTS

The author expresses his sincere thanks to K. Fukushima, T. Matsui, O. Morimatsu, K. Ohnishi, M. Ohtani for fruitful discussions and to the members of Komaba nuclear theory group for their interests on this subject. This work is supported in part by the Grants-in-Aid for Scientific Research of Monka-sho (Grant No. 13440067).

---

[1] M. Asakawa and K. Yazaki, Nucl. Phys. **A504** 668,1989.
[2] S. Gavin, A. Gocksch, R.D. Pisarski, Phys. Rev. D **49** 3079, 1994 (hep-ph/9311350).
[3] J. Berges and K. Rajagopal, Nucl. Phys. **B538** 215, 1999 (hep-ph/9804233).
[4] M.A. Halasz, A.D. Jackson, R.E. Shrock, M.A. Stephanov, and J.J.M. Verbaarschot, Phys. Rev. D **58** 096007, 1998 (hep-ph/9804290).
[5] Z. Fodor and S.D. Katz, JHEP 0203, 014,2002 (hep-lat/0106002).
[6] M.A. Stephanov, K. Rajagopal and E.V. Shuryak, Phys. Rev. Lett. **81** 4816,1998 (hep-ph/9806219).
[7] M.A. Stephanov, K. Rajagopal and E.V. Shuryak, Phys. Rev. D **60** 114028,1999 (hep-ph/9903292).
[8] S. Gavin, nucl-th/9908070.
[9] B. Berdnikov and K. Rajagopal, Phys. Rev. D **61** 105017, 2000.
[10] O. Scavenius, A. Mocsy, I.N. Mishustin and D.H. Rischke, Phys. Rev. C **64** 045202, 2001 (nucl-th/0007030).
[11] S. Borsanyi, A. Patkos, D. Sexty, Z. Szep, Phys. Rev. D **64** 125011, 2001 (hep-ph/0105332).
[12] Y. Hatta and T. Ikeda, Phys. Rev. D **67** 014028, 2003 (hep-ph/0210284).
[13] K. Fukushima, Phys. Rev. C **67** 025203 (hep-ph/0209270).
[14] Y. Hatta and M.A. Stephanov, hep-ph/0302002.
[15] T. Hatsuda and T. Kunihiro, Phys. Rept. **247** 221, 1994.
[16] S.P. Klevansky Rev. Mod. Phys. **64** 649, 1992.
[17] P.C. Hohenberg and B.I. Halperin, Rev. Mod. Phys. **49** 435, 1977.
[18] H. Fujii, K. Ohnishi, and M. Ohtani, in preparation.
[19] Y. Nambu and G. Jona-Lasinio, Phys. Rev. **122** 345, 1961; **124** 246, 1961.
[20] T. Kunihiro, Phys. Lett. **B271** 395, 1991.
[21] A. Gocksch, Phys. Rev. Lett. **67** 1701, 1991.
[22] H.E. Stanley, *Introduction to phase transitions and critical phenomena*, Oxford (1977).

[23] I. Lawrie and S. Sarbach, in *Phase Transitions and Critical Phenomena*, ed. by C. Domb and J. Lebowitz (Academic Press, NY, 1984), Vol. 9, pp. 1.
[24] T. Hatsuda and T. Kunihiro, Phys. Rev. Lett.**55** 158, 1985.
[25] M. Kitazawa, T. Koide, T. Kunihiro and Y. Nemoto Phys. Rev. D **65** 091504(R), 2002 (nucl-th/0111022).
[26] A. Patkos, Z. Szep and P. Szepfalusy, Phys. Rev. D **66** 116004, 2002 (hep-ph/0206040).
[27] Y. Hidaka, O. Morimatsu and T. Nishikawa, hep-ph/0211015.
[28] M. Le Bellac, *Thermal Field Theory*, Cambridge University Press (1996).
[29] K. Ohnishi and M. Ohtani, private communications.
[30] K. Fukushima, private communications.
[31] A.L. Fetter and J.D. Walecka, *Quantum Theory of Many–Particle Systems*, McGraw Hill (1971).
[32] L. van Hove, Phys. Rev. **95** 249;1374, 1954.
[33] M. Asakawa, U. Heinz and B. Muller, Phys. Rev. Lett. **85** 2072, 2000 (hep-ph/0003169).
[34] S. Jeon and V. Koch, Phys. Rev. Lett. **85** 2076, 2000 (hep-ph/0003168).
[35] D. Bower and S. Gavin, Phys. Rev. C **64** 051902, 2001 (nucl-th/0106010).